

Development of Program for Synchronous Processing of Surface ECG and Intracardiac Electrograms

Aleksei Anisimov^{1,2}, Timofey Sergeev¹, Alena Skorobogatova²

¹Institute of Experimental Medicine FSBSI "IEM", Saint-Petersburg, Russia

²Saint-Petersburg Electrotechnical University "LETI", Saint-Petersburg, Russia

aanisimov@etu.ru, stim9@yandex.ru, alenskorobogatova@gmail.com

Abstract—This article describes the development of a software-algorithmic complex that allows processing synchronous recordings of surface electrocardiograms and intracardiac electrograms. The developed software allows visual assessment of signals, an automated analysis of records, determining characteristic points of single signals and their joint parameters, building a classification model on their basis. Database of synchronous recordings of electrograms and electrocardiograms from patients with cardiovascular disorders was created and used for successfully approbation of developed software.

I. INTRODUCTION

The cardiac conducting system (CSS) consists of the structures able to spontaneously get excited and conduct electrical signals [1]. Normally, the pacemaker is the sinoatrial node (SA-node). Its discharge frequency is about 70 beats per minute at rest [2]. The excitation appears in the SA-node and propagates through the Bachmann bundle, the longitudinal bundles the atrioventricular node, which is located in the atrioventricular septum finally reaching the bundle of His causing excitation of the ventricles. The bundle of His is divided into left and right legs, which branch and end with Purkinje fibers. These fibers transmit excitation directly to the myocardium [3]. If this normal conduction way is disturbed the excitation propagates through new, “pathological” pathways [4].

The body-surface 12-lead ECG usually provides information about the presence of cardiovascular disorders and clarifies their nature. However, some disturbances could be inconstant (e.g. short fibrillations or atrial flutter) and do not reveal themselves on the common ECG. In this case it is helpful to put in the heart probe electrodes and get electrograms of various structures of the CSS. These electrograms show if there is a conductivity in the interested myocardium area and help to determine where the pathway is disturbed.

To register bundle of His electrogram the probe electrode is put near the tricuspid valve. By determining an interval between the wave of depolarization of the atria and the bundle of His which called the AN interval (60–125 ms normally) it is possible to estimate the conducting time in the AV-node. Another interval usually determined is between the wave of depolarization of the His bundle and the beginning of the QRS complex (ventricular contraction) on the ECG or an interval to V-wave on the electrogram signal. This interval is called HV (35–55ms normally). Using this interval, the conducting time in the His- Purkinje fibers system is estimated [5].

To record the electrical activity of the SA-node, the electrode is placed at the site of the vena cava entering the right atrium. For the left atrium the electrogram is recorded either directly or indirectly from the coronary sinus.

Synchronous recording of the described electrograms allows determining the localization of areas with conduction disturbances both atrial and ventricular.

Information obtained from the analysis of the body-surface ECG helps to determine the type of a pathology: intracardiac conduction disturbance and arrhythmias. However, electrogram signals recorded in various parts of the heart provide more accurate information about pathology including its source and localization. Thus, a joint analysis of the ECG and intracardiac electrograms allows to carry out more complete cardiovascular system condition analysis.

The impulses are carried out with the help of cardiomyocytes, which are the structural unit of the heart muscle. ECG phase changes ratios and cardiomyocyte electrogram are shown in Fig. 1 [6].

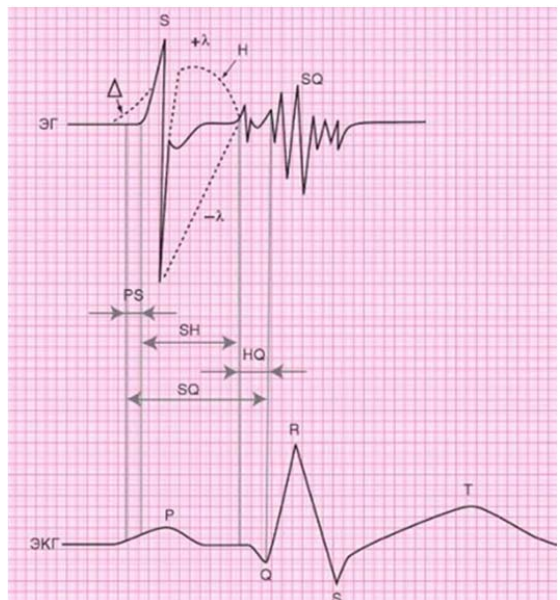


Fig.1. ECG phase changes ratio and electrogram cardiomyocytes: S – atrium spike excitation at the location of the stimulating electrode; H – potential of bundle branch on electrogram; QRS – ventricular complex of the electrocardiogram; T – T spike on ECG; λ is the deviation of the atrioventricular interval; P-S – interval between the beginning of the P spike (ECG) and atrial spike (the electrogram); S-H – interval between the atrium spike (the electrogram) and the potential of bundle branch, H-Q(R) is the interval of GIS ventricle; S-Q(R) – atrioventricular interval (electrogram).

Simultaneous synchronous registration of surface ECG and intracardiac electrograms of different parts of the heart allows to determine the localization of conduction disorders of heart structures. So while pathologies aren't always visible on normal signal of superficial ECG, intracardiac electrogram signals can reveal pathological signs.

Common body-surface ECG and intracardiac electrogram can also be recorded for signals containing pathological parts. In this case the localization of pathology can be determined for certain. Fig. 2 shows a pathological ECG with the extrasystole called bigemina. Body-surface ECG shows the presence of a disturbance but it is impossible to establish the localization of the arrhythmogenic zone. However, intracardiac electrograms recorded synchronously with ECG allow to determine that the source of an arrhythmia is the sinus node for complexes 1–5 and the trunk of the AV-node or bundle of His for complexes 6 and 7. Thus, a joint analysis of ECG and intracardiac electrogram signals provides significantly more information than using only ECG and expands the diagnostic capabilities of electrocardiography.

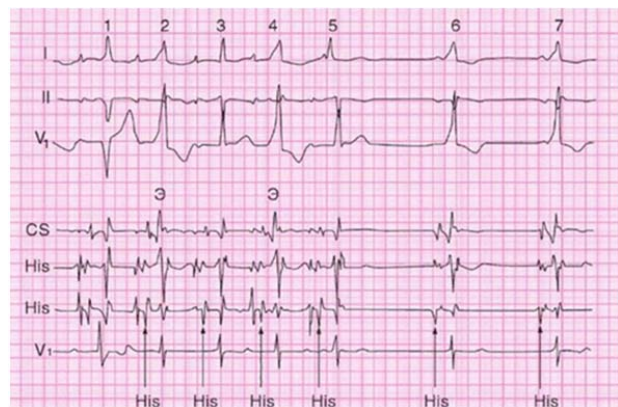


Fig.2. Synchronous recording of surface ECG and intracardiac electrograms for a patient with extrasystole

Obtaining intracardiac electrograms is very complicated, which is the main problem of the method. Recording data is possible only in the operating room and it is a standard practice providing many opportunities for research.

II. SIGNAL ACQUIRING METHOD

Signals registration takes place during radiofrequency catheter ablation (RFA) and electrophysiological examination (EFI) in the surgical Department. RFA of the heart is a surgical intervention in which the patient is punctured through the femoral artery and catheters are inserted into the heart

cavity. Through the use of radiofrequency energy heart rhythm disturbances and intracardiac conduction are eliminated. This method is one of the most modern treatment methods for most types of cardiac arrhythmias and intracardiac conduction. These operations are referred to as minimally invasive interventions. RFA is rarely performed on the open heart [7], [8].

The RFA procedure is performed under local anesthesia. After the probes are inserted through the femoral artery of the patient, pathological activity is studied by recording electrograms from different sites using multipolar catheters-electrodes. The electrodes can be used both to record electrical activity and to conduct electrical stimulation of the whole heart to initiate and arrest the disorder. To control the location of catheters, operations are performed under x-ray.

A number of catheters-electrodes are used to register electrograms of different sites, each performs its own function. The catheters used are listed below.

- Ablative catheter electrode (ABL) consists of 4 electrodes, which form 2 leads: distal and proximal. These leads detect activity perpendicular to each other. One lead is located at the tip of the catheter, the second at a short distance from it.
- Catheter-electrode, placed in the coronary sinus (CS). This catheter contains 10 electrodes, arranged in pairs with a constant step from each other, resulting in five consecutive leads from the tip and deep into the catheter. Information from the coronary sinus electrodes allows to determine the sequence of excitation propagation in the structures of the heart during delay events to draw conclusions about the presence of pathologies. Also, in rare cases, these electrodes can be used for electrical stimulation and to determine the conductivity of the myocardial site (playing the role of the reference electrode).
- Lasso catheter electrode. This electrode contains 10 pairs of electrodes, which form 10 consecutive leads, located from the tip of the catheter to its insides. The catheter is twisted into a double-layered ring located at the end of the pulmonary veins. These electrodes often used in case of atrial fibrillation, the main source of which are conductive areas arising at the confluence of veins. The purpose of such a catheter is to search for conductive areas (using an ablative electrode, lasso catheter electrodes are reference) and their stimulation to check the isolation.

Signals, registered during atrial fibrillation elimination, are shown on Fig. 3

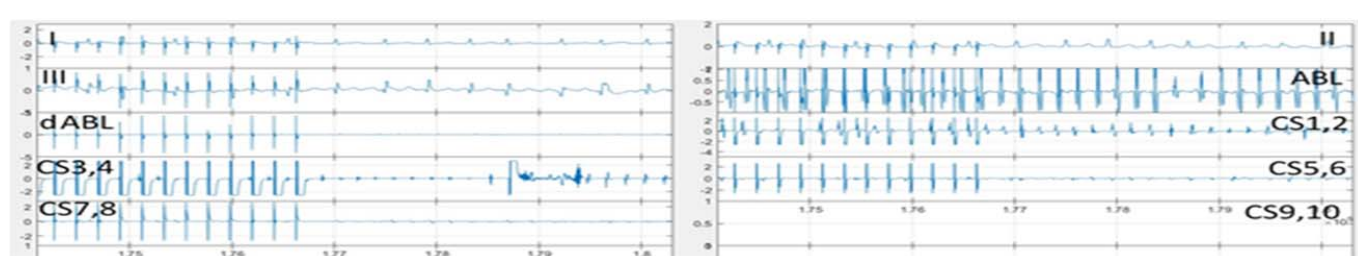


Fig. 3. Signals received during atrial fibrillation elimination

III. ALGORITHM DESCRIPTION

The developed algorithmic complex is designed to simplify the work of the doctor, eliminating the need for manual corrections and measurements. The initial stage of the algorithm is the pre-processing of signals, designed to highlight the informative part of the signal against the background noise and artifacts, namely digital filtering.

After the signal preprocessing characteristic points of the surface ECG and the intracardiac electrogram are detected. These points indicate the start and end phases of cardiac contraction: systole and diastole of atria and ventricles. Characteristic points location is determined by means of the threshold algorithms based on finding of a derivative. All uninformative frequencies are filtered out at this stage to increase method stability.

During the first step, the main or reference point is located. For the surface ECG this is the position of the R-wave; for intracardiac electrograms – the position of the first peak and the beginning of activity. Between found control points the remaining characteristic points are determined with reference to the main points for correct delays determination. After the characteristic points are found, time delays between the selected events are calculated. The amplitude parameters are also calculated, but they have greater variability for a particular record.

The calculated parameters are displayed on the graphs. They also provide initial data for constructing a classification model of violation type. The scheme of the developed algorithmic complex is shown in Fig. 4.

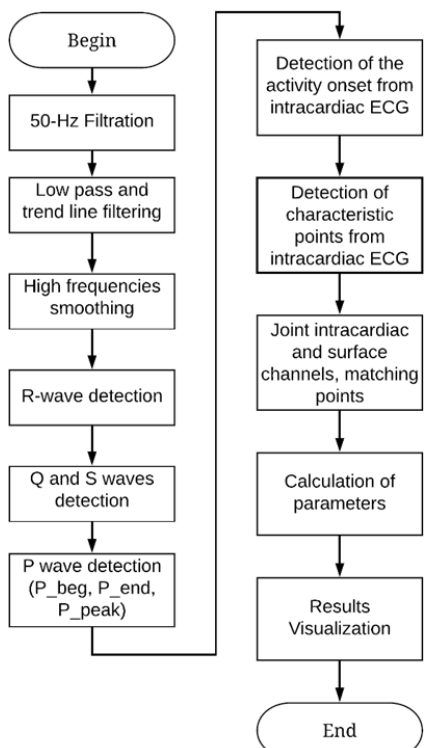


Fig. 4. Algorithm for synchronous processing of electrocardiogram signals and intracardiac electrograms

After preliminary processing of the cardiac signal, the characteristic points of the signal are determined. At the first stage, there is a selection of reference points: the QRS-complex, showing the contraction of the heart ventricles and reflecting the depolarization potential. The frequency of QRS-complex lies between 8 and 24 Hz [9]. A modified pan Tompkins algorithm based on the analysis of the derivative of the surface ECG signal is used to detect the R-wave (which has the maximum power among all components of the QRS complex) [10].

After determining the reference points corresponding to the R wave, the remaining characteristic points of the surface ECG signal are selected. At first points corresponding to waves Q and S are allocated. Phase Q determination takes place in the 12 ms section prior to the corresponding R-wave in this area. The signal is filtered with a subsequent search of the zero of the derivative. The S wave is searched in a similar wave, but the search is conducted to the right of the R-wave. Next, there is a selection of the wave that occurs during atrial depolarization, P-wave, with a frequency of 5 to 10 Hz.

Extraction of the P-wave occurs in several stages in accordance with the method proposed by Hengeveld and van Bemmel [11], the ECG signal goes through the following stages of processing:

1. Removal of QRS-complexes. After the detection of QRS-complexes using the previously described algorithm, found complexes are replaced by a baseline determined by the analysis of samples preceding the QRS-complex. This stage of the algorithm makes it possible to exclude the dominant influence of the QRS-complex, against which the definition of the P-wave becomes more complex.

2. Filtering the resulting signal. To allocate the frequency band corresponding to the P-wave, the signal is filtered using a bandpass filter with a bandwidth equal to 3-11 Hz.

3. QT interval calculation. The search for the P-wave occurs in the interval determined according to formula (1).

$$QT_{max} = 2.9 * RR + 250 \text{ ms}, \quad (1)$$

RR is the interval between adjacent R-waves (two consecutive QRS complexes). QT is calculated in all leads (three to twelve, usually three). Next, the maximum and minimum QT values are determined, as well as the final QT interval.

4. Absolute value calculation. At a certain QT interval, the resulting signal is taken modulo. Within the QT interval, the maximum value of the signal is also determined.

5. Threshold calculation. Thresholds with levels of 50% and 75 % of the maximum defined in the QT interval are calculated. These values are used to determine the three-level signal, which is a simplified sample of the P-wave. This three-level signal is used to determine the position of the P-wave.

6. Finding cross-correlation between the resulting signal and the sample of the P-wave. The maximum of this function corresponds to the position of the P-wave in the original ECG. A simpler threshold algorithm for finding extrema (using a

derivative) is also used to determine the positions of the P-wave. The result of the P-wave search algorithm is shown in Fig. 5.

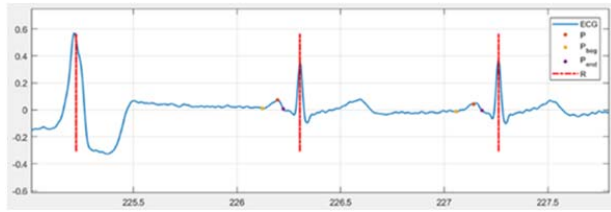


Fig.5. ECG signal with detected P and R waves

To determine the parameters of the intracardiac electrogram signal, the characteristic points of the signal corresponding to the extreme values of the signal section are searched. The first step is to determine the main, reference signal point. In this case, such a reference point is the beginning of the reduction, which is characterized by a sharp change in the speed of the signal, which can be easily fixed by the signal derivative. Determination of the beginning of activity is performed using stages, almost similar to the stages of QRS-complexes allocation. The remaining characteristic points of the intracardiac electrogram are distinguished by simple threshold algorithms for finding extrema based on the analysis of the signal derivative. As a result of the algorithm, the points of the first and second maxima, as well as the point of the first minimum are allocated. The result of the detection of the characteristic points is shown in Fig. 6, where the numeral 1 indicates the beginning of electrical activity, 2 – first maxima, under the number 3 is the first minimum and the numeral 4 is the second maximum.

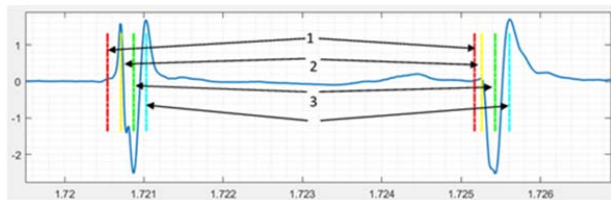


Fig. 6. Characteristic points of the intracardiac electrogram

IV. JOINED PROCESSING OF SURFACE CARDIOGRAMS AND INTRACARDIAC ELECTROGRAM

As a result of the search for characteristic signal points, each complex should correspond to several points at once. To establish the correspondence between the found points and the various leads of the surface ECG, in which these points were isolated, the search for a per-channel correspondence of the complexes takes place. The reference points in this case are the selected QRS-complexes, since this wave is one of the main characteristics of the cardiac signal. To get into the final marking, it is necessary to confirm the selected complex by at least one more lead. If the selected wave has not been confirmed, it is rejected (along with other points) and excluded from the analysis in order to avoid false positive errors.

Similarly, the correspondence between the points of the surface ECG and the intracardiac electrogram is established. Binding of points to one time event (in this case R-wave) is a prerequisite for further time and amplitude parameters

calculation. The parameters found from the signals of the intracardiac electrogram are divided into two groups: atrial (atr) and ventricular (vent). Results of establishing the conformity of the characteristic points of the various leads to each other is presented in Fig. 7, where numeral 1 shows a surface ECG signals, and the numeral 2 – intracardiac electrogram from the electrode installed in the coronary sinus, 159 on the chart corresponds to the number of the record.

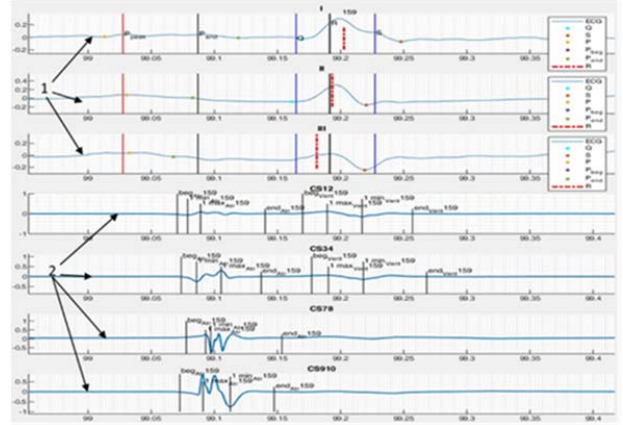


Fig. 7. Result of the joint allocation of points on the surface ECG signal (1) and intracardiac electrograms (2)

After selecting feature points and binding points of various leads to a particular heart contraction, calculation of the followed parameters takes place.

Surface cardiogram parameters:

- Duration of P-wave (p_dur) equal to the difference between the time of the end (P_end), and the start (P_beg) of P-wave, in seconds;
- Duration of QRS complex (qrs_dur) equal to the time difference between S and Q waves, in seconds;
- Interval QR (qr_dur) found as a time difference of waves R and Q, in seconds;
- Interval PQ (pq_dur), calculated as the time between the end of wave P (P_end) and the beginning of QRS (point Q), in seconds;
- Absolute amplitude of the wave P (p_val), measured from the value of the signal surface ECG at the beginning of P-wave and its maximum;
- Average speed of QR, calculated as the median value of the derivative in QR section;
- Average speed of P, calculated as the median value of the derivative in ($P_peak - P_end$);

Intracardiac electrogram parameters:

- Duration of the atrial activity ($atrAct_dur$) equal to the time passed from the selected starting point of the activity of the Atria (beg_atr) to the point of end of activity of the Atria (end_atr), in seconds, the same parameter is calculated in the same way and to the ventricles ($ventAct_dur$);
- Time elapsed from the start of activity to the first maximum ($begMx_dur$) is determined for both atrial and ventricular activity and is measured in seconds;

- Time elapsed from the first minimum to the end of activity (`mnEnd_dur`) is determined for both atrial and ventricular activity in seconds;
- Number of peak values from the start of activity to the end of activity (`Npeaks`), with the difference between the maximum and minimum values of at least 25 % of difference between the first minimum and the first maximum. This parameter is determined for the areas of atrial and ventricular activity;
- Relative magnitude between the end point of the activity and the first minimum (`endMn_val`), this value is calculated for atrial and ventricular activity;
- Average speed in the area between the first minimum and maximum, defined as the median derived at the site (`MxMn_med`), this parameter is also calculated for all types of activity;
- Time from the end of atrial activity until the beginning of the ventricular (`eAtrbVent_dur`), this is a joint parameter for the two types of activities and measured in seconds;
- Time from beginning of atrial activity until the beginning of the ventricular (`bAtrbVent_dur`), this is a joint parameter for the two types of activities and measured in seconds;
- Ratio of the span of `begMx_val` of the ventricles to `begMx_val` of the atria (`rangeBegMx`);
- Ratio of the span of the `endMn_val` of the ventricles to the `endMn_val` of the atria (`rangeEndMn`).

Joint parameters of a surface ECG and intracavitary electrogram:

- Length of the section from the onset of atrial activity on the surface ECG and intracavitary electrogram (`jBegsAtr`) and the delay between the onset of ventricular activity on the surface ECG and intracavitary signal (`jBegsVent`), both parameters are measured in seconds;
- Delay between the end of activity on a surface ECG and intracavitary electrogram for atria (`jEndsAtr`) and ventricles (`jEndsVent`), determined in seconds;
- Time between the maximum atrial activity on the surface ECG (`P_peak`) and the first maximum of atrial activity of the intracavitary electrogram (`1Mx`), `jPMx_dur`, measured in seconds;
- Time between the maximum ventricular activity on the surface ECG (`R`) and the first maximum ventricular activity of the intracardiac electrogram (`1Mx`), `jRMx_dur`, is measured in seconds.

As a result of calculating these parameters, a matrix of covariance of attributes was constructed, which allows us to analyze the dependence of the attributes on each other. As a result of such analysis, we can find signs that are highly dependent on each other. The inclusion of such a pair of attributes in the analysis will not only increase the complexity of the model, but may also worsen its predictive ability (due to the fact that only one attribute from the pair is informative). Therefore, due to the analysis of the covariance matrix, we can conclude that there are signs that can be excluded from the analysis based on the strong relationship between them. The covariance matrix is shown in Fig. 8.

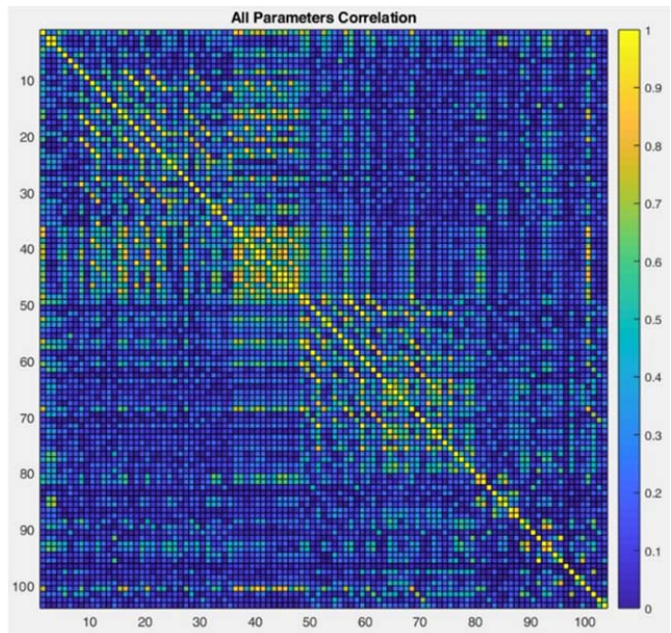


Fig. 8. Covariance matrix

To assess the intersection of the three classes (atrial fibrillation, atrial flutter, and normal rhythm), histograms of distributions were constructed for each of the described attributes, and the values of the Fisher criterion for each symptom were calculated using equation (2).

$$J = \frac{(m_1 - m_2)^2}{(\sigma_1^2 + \sigma_2^2)} \quad (2)$$

where m_1 and m_2 are the mean values of the sample distributions of the corresponding attributes of the first and second classes, respectively, σ_1 and σ_2 are the mean square deviations of the attributes of the first and second classes.

Based on the analysis of the obtained histograms, Fisher values, as well as the estimation of the covariance matrix, ten parameters were selected. The values of the Fisher criterion for which were of the greatest importance (which indicates the ability to separate selected classes for this attribute), a visual analysis of the histograms of these attributes also confirmed these assumptions. The correlation coefficient for the selected attributes should not exceed 0.85, in some cases 0.75.

Thus, carrying out the data of calculations and analysis of each feature allows to conduct a comparative analysis and conclude which attributes are the most informative, or, conversely, uninformative. Identification of informative attributes can reduce the possibility of creating a redundant model, reduce its complexity, as well as the number of necessary calculations.

Table I shows the obtained statistical estimates for the distribution of the selected attributes and the corresponding values of the Fisher criterion for classes 1, 2, 3 (atrial fibrillation, atrial flutter, and normal rhythm, respectively).

TABLE I. CALCULATED STATISTICAL PARAMETERS

Attribute	σ_1	σ_2	σ_3	m_1	m_2	m_3	J_{12}	J_{13}	J_{23}
atrAct_durCS34	0,02	0,007	0,007	0,07	0,13	0,07	6,16	0,001	7,63
atrNpeaksCS12	0,83	0,52	0,51	2,55	3,75	3,19	1,50	0,43	0,60
atrNpeaksCS34	0,76	0,52	0,51	1,29	2,53	2,28	1,82	1,15	0,12
atrBegMxValCS12	0,23	0,10	0,05	0,34	0,16	0,18	0,54	0,49	0,03
atrBegMxValCS34	0,03	0,07	0,38	0,04	0,24	0,64	6,53	2,48	1,06
atrEndMnValCS12	0,25	0,21	0,06	0,81	0,49	0,27	0,91	4,33	1,04
atrEndMnValCS34	0,04	0,05	0,16	0,10	0,34	0,88	12,71	21,25	9,85
atrMxMn_CS34	0,003	0,007	0,10	0,003	-0,02	0,08	12,29	0,56	1,05
vnBgMx_ValCS12	0,31	0,09	0,05	0,38	0,20	0,05	0,34	1,13	2,07
vnBegs_j_CS12	39,3	10,19	17,05	15,35	-16,48	42,54	0,62	0,40	8,83

After a visual assessment of the distributions of class objects in the space of all attributes, the dependence of the signs among themselves was evaluated. Fig. 9 shows the covariance matrix, showing the degree of dependence of the features from each other.

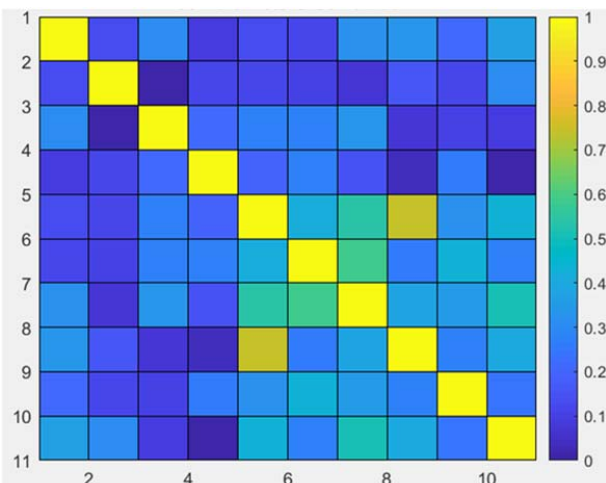


Fig. 9. Covariance matrix

As a result of the analysis of the results, it was decided to reduce the dimension of the feature space, to simplify the model, and also to exclude from the analysis the most uninformative features (dependent or having poor ability for separation for the selected classes). To further build the classification model, the following features were selected:

- atrAct_durCS34;
- atrNpeaksCS34;
- atrBegMxVal_CS12;
- atrMxMn_CS34.

According to these characteristics, a cluster analysis was made by using the hierarchical clustering method, the distance was calculated using the ward method.

As a result of the work of the algorithmic complex, a model was created for joint analysis, as well as determination of characteristic points and parameters of surface ECG signals and intracavitary electrogram signals. The accuracy assessment of the characteristic point detection algorithms was evaluated using a database of records, which were obtained during operations (radiofrequency catheter ablation) in The Almazov National Medical Research Centre for patients with cardiac arrhythmias. During all operations continuous signals, that reflect cardiovascular activity, were recorded. The number of electrodes, as well as recorded leads may vary depending on the type of pathology under study.

As a reference (the “gold standard”), the values obtained using manual markings of the described files were used. Moreover, it should be noted that the resulting marking obtained as a result of combining several channels (for a surface ECG) is compared with reference values.

Highly noisy areas were deleted during manual marking, based on the technical specifications for creating an algorithm that did not imply the operation of the algorithm on highly noisy areas.

According to the results of the work, we obtained the accuracy values of the algorithms shown in Table II and Table III. Where FP (false positive) is the number of false positive errors, FN (false negative) is the number of false negative values, TP (true positive) is the number of truly positive values (number of points, which should have been detected on this signal). Usually, TN (true negative) values are also calculated – true negative values, but due to the statement of the problem, such values either cannot be determined, or they should be taken as 100%, which is not entirely correct. Therefore, in

determining the accuracy of the algorithm in this problem, the sensitivity value (Se) and the value p+ (positive predictive value) were used, that is, the positive predictive value of the algorithm.

TABLE II. INDICATORS OF INTRACARDIAC ELECTROGRAM POINTS DETECTION ACCURACY

Points	FP	FN	TP	Se, %	P+, %
Q	74+114 (III)	178	2852	94,13	97,74
R	82+114 (III)	166	2864	94,52	97,22
S	76+114(III)	179	2851	94,09	97,40
P-wave begin	39	373	904	70,79	95,86
P-wave end	42	357	920	72,04	95,63
P_peak	44	346	931	72,90	95,48

TABLE III. INDICATORS OF INTRACARDIAC ELECTROGRAM POINTS DETECTION ACCURACY

Points	FP	FN	TP	Se, %	P+, %
Q	54	185	2850	93,90	98,14
R	63	176	2879	94,23	97,85
S	56	186	2863	93,90	98,08
P-wave begin	31	375	908	70,77	96,70
P-wave end	34	356	923	72,17	96,45
P_peak	35	352	931	72,56	96,38

Based on the analysis of Table II and Table III, we can conclude that the application of the operation of converting several channels of the surface ECG into the general markup can reduce false positive errors and increase the specificity of the algorithm (due to the need to confirm one channel by others). However, when using this operation, it leads to an increase in the number of false negative errors and lower sensitivity of the algorithm. Thus, the use of the markup combining operation allows to prevent overdiagnosis by reducing the sensitivity of the algorithm, but increasing confidence at a specific point on the surface ECG signal. In addition, when applying the operation of combining channel-by-channel markings, it helps to avoid cases of complete absence of the algorithm triggering on a particular channel. Therefore, the application of the operation of mixing channel-by-channel markings into one allows analyzing cardiac activity in the area, based on information from several channels at once.

The accuracy of the Pan-Tompkins algorithm is 98% based on the results. The difference in 4.5% of the value obtained in practice from the theoretically obtained value is explained by the fact that signals with different pathologies (or even without them) were used, and the difference can arise due to the presence of rounding errors.

The accuracy of determining P-wave based on the logic of

constructing the algorithm depends on the accuracy of determining the QRS complexes, since for the search of P-waves the QRS complex will be replaced by the baseline.

After identifying the characteristic points of the signals, the joint parameters of the signals are calculated, and cluster analysis (based on these parameters) is used to build a model that allows separating objects for three classes: atrial fibrillation, atrial flutter, and normal rhythm. As a result of using this model, based on the recorded signals of patients with cardiac impairment, the results of clustering of objects into 3 classes were obtained: atrial fibrillation (AF), atrial flutter (AF) and normal rhythm (NR), presented in Table IV, similar to Table II and Table III (all designations coincide).

TABLE IV. INDICATORS ACCURACY

Classes	FP	FN	TP	Se, %	P+, %
AF	290	85	555	86,72	65,68
AF	175	208	518	71,35	74,75
NR	73	97	545	84,89	88,19

V. CONCLUSION

Based on the analysis of Table IV, it is clear that the number of truly positive results is quite large, which proves the efficiency and applicability of this method. There is also a relatively large number of false positive and false negative errors for pathology classes, however, detecting the normal rhythm class showed a sensitivity and specificity of the method of at least 85%, which is a good result and indicates the applicability of this method with adjustments.

The development of the algorithmic complex included several stages: design of algorithm scheme and the processing steps, theoretical justification of the methods used, the preliminary processing (filtering), the selection of characteristic points of the surface ECG signal, the implementation of the algorithm for combining channel-based markings of the surface ECG (in several leads) into one. The same stages were made for intracardiac electrograms: selection of characteristic points, calculation of the joint parameters of the signals and their analysis. The analysis was carried out using the cluster analysis method, which resulted in the task of separating signal sections into 3 classes (atrial fibrillation, atrial flutter and normal rhythm).

As a result of the analysis of existing signal databases, it was found that only one database of joint ECG and intracardiac electrogram recordings is presented on modern open resources. Due to this fact, it was decided to create a verified database in which a larger number of pathologies will be presented. Such a base was collected on the basis of The Almazov National Medical Research Centre for patients with cardiac arrhythmias. Software-algorithmic complex that allows the joint analysis of surface ECG signals and intracardiac electrograms was created in the MATLAB software environment. The developed software package is convenient, intuitive, and also easily customizable for the needs of a specific clinician.

ACKNOWLEDGMENT

This study was supported by the Russian Foundation for Basic Research, Grant № 18-29-02036.

REFERENCES

- [1] Kushakov M.S., *Arrhythmias of the heart*. St. Petersburg, 1999.
- [2] Karpov V.A., Conducting heart system. *Almanac of young science*, № 1, pp. 48–49.
- [3] Krylova N.V. *Anatomy of the heart in tables and diagrams*. Moscow: Medical News Agency, 2008.
- [4] Sinelnikov, R.D. *Atlas of human anatomy. In 4 volumes*. Moscow.: Medicine, 2006.
- [5] Ardashev A.V. et al, Radiofrequency ablation of non-ischemic ventricular rhythm disturbances in the immediate vicinity of the His bundle. *Bulletin of Arrhythmology*, V. 42, 2006, pp. 28-34.
- [6] Murashko V.V., Strutinsky A.V. *Electrocardiography: textbook allowance*. Moscow: Medpress-inform, 2017 .
- [7] Darrieux F. C. C., Scanavacca M. I., Hachul D. T. et al, Radiofrequency catheter ablation of premature ventricular contractions originating in the right ventricular outflow tract. *Arg. Bras. Cardiol*, Vol. 88 (3), 2007, pp. 236-243.
- [8] Di Biase L., Burkhardt J.D., Lakkireddy D. et al, Mapping and ablation of ventricular arrhythmias with magnetic navigation: comparison between 4- and 8- mm catheter tips. *J. Interv. Card. Electrophysiol.*, Vol. 26 (2), 2009, pp. 133–137.
- [9] Benitez D. S., Gaydecki P. A., Zaidi A., Fitzpatrick A. P. A, New QRS Detection Algorithm Based on the Hilbert Transform. *IEEE Computers in Cardiology*, 2000, pp. 379–383.
- [10] Oweis R.J., Al-Tabbaa B.O. QRS Detection and Heart Rate Variability Analysis: A Survey. *Biomed. Sci. and Eng.*, Vol. 2, No. 1, 2014, pp. 13–34.
- [11] Hengeveld S. J. and van Bemmel J. H. Computer detection of P waves . *Comput. Biomed. Res.*, V. 9, pp. 125–132.